Fast-Moving Structures in the Debris Disk Around AU Microscopii

Anthony Boccaletti[1], Christian Thalmann[2], Anne-Marie Lagrange[3,4], Markus Janson[5,11], Jean-Charles Augereau[3,4], Glenn Schneider[6], Julien Milli[7,4], Carol Grady[8], John Debes[9], Maud Langlois[10], David Mouillet[3,4], Thomas Henning[11], Carsten Dominik[12], Anne-Lise Maire[13], Jean-Luc Beuzit[3,4], Joe Carson[14], Kjetil Dohlen[15], Markus Feldt[11], Thierry Fusco[16,15], Christian Ginski[17], Julien H. Girard[7,4], Dean Hines[9], Markus Kasper[18,4], Dimitri Mawet[7], François Ménard[19], Michael Meyer[2], Claire Moutou[15], Johan Olofsson[11], Timothy Rodigas[20], Jean-Francois Sauvage[16,15], Joshua Schlieder[21,11], Hans Martin Schmid[2], Massimo Turatto[13], Stephane Udry[22], Farrokh Vakili[23], Arthur Vigan[15,7], Zahed Wahhaj[7,15], John Wisniewski[24]

May 18, 2015

Giant planets form in disks of gas and dust that surround newborn stars, over timescales of a few million years. Some stars retain a dust disk significantly longer, which is taken as evidence for an unseen population of asteroid-like bodies (planetesimals) whose destructive collisions continually replenish the system with dust[1]. Such debris disks serve as valuable observational markers of planet formation and can reveal additional clues to the presence of planets in the form of eccentric, clumpy or warped features[2–4]. The nearby, young star AU Microscopii (AU Mic) hosts a well-studied gas-poor debris disk in which earlier imaging studies detected signs of asymmetric structures[5–8]. Here we present the discovery of large-scale structures in the AU Mic debris disk obtained with the newly commissioned SPHERE planet-finder instrument at the Very Large Telescope[9]. The structures comprise five wave-like arches at projected separations of 10–60 au from the star. Comparison with re-processed images from Hubble Space Telescope (HST) data taken in 2010 and 2011[10] allows us to track the location of these features over a 4-year baseline, revealing systematic motion away from the star at projected speeds of 4–10 km/s. This exceeds system escape velocity for at least three of the five features, ruling out conventional disk features caused by gravitational perturbers like planets. Given the lack of theoretical and observational precedent for such structures, their origin remains an open question, though the star's known flaring activity is likely involved.

In the nineteen-eighties, infrared (IR) excess emissions were discovered around main-sequence stars[1].

[1]LESIA, Observatoire de Paris, CNRS, Université Paris Diderot, Université Pierre et Marie Curie, 5 place Jules Janssen, 92190 Meudon, France
[2]ETH Zürich, Wolfgang-Pauli-Strasse 27, CH-8093 Zürich Switzerland
[3]Université Grenoble Alpes, IPAG, F-38000 Grenoble, France
[4]CNRS, IPAG, F-38000 Grenoble, France
[5]Department of Astronomy, Stockholm University, Stockholm, Sweden
[6]Steward Observatory, 933 North Cherry Avenue, The University of Arizona Tucson, AZ 85721, USA
[7]European Southern Observatory (ESO), Alonso de Córdova 3107, Vitacura, Casilla 19001, Santiago, Chile
[8]Eureka Scientific, 2452 Delmer, Suite 100, Oakland CA 96002, USA
[9]Space Telescope Science Institute, 3700 San Martin Dr. Baltimore, MD 21218, USA
[10]Centre de Recherche Astrophysique de Lyon, (CNRS/ENS-L/Université Lyon1), 9 avenue Charles André, 69561 Saint-Genis-Laval, France
[11]Max-Planck-Institut für Astronomie Königstuhl 17, D-69117 Heidelberg, Germany
[12]University of Amsterdam Sterrenkundig Instituut "Anton Pannekoek" Science Park 9041098 XH Amsterdam, the Netherlands
[13]INAF-Osservatorio Astronomico di Padova, Vicolo dellOsservatorio 5, 35122, Padova, Italy
[14]Department of Physics & Astronomy College of Charleston, USA
[15]Aix Marseille Université, CNRS, LAM (Laboratoire dAstrophysique de Marseille) UMR 7326, 13388, Marseille, France
[16]ONERA - The French Aerospace Lab, 92322, Châtillon, France
[17]Sterrewacht Leiden, PO Box 9513, Niels Bohrweg 2, NL-2300RA Leiden, the Netherlands
[18]European Southern Observatory (ESO), Karl Schwarzschild Strasse, 2, 85748 Garching bei München, Germany
[19]UMI-FCA, CNRS/INSU, France (UMI 3386), and Dept. de Astronomía, Universidad de Chile, Santiago, Chile
[20]Department of Terrestrial Magnetism, Carnegie Institution of Washington, 5241 Broad Branch Road, NW, Washington, DC 20015, USA
[21]NASA Postdoctoral Program Fellow, NASA Ames Research Center, Space Science and Astrobiology Division, MS 245-6, Moffett Field, CA, 94035, USA
[22]Observatoire de Genève, University of Geneva, 51 Chemin des Maillettes, 1290, Versoix, Switzerland
[23]Laboratoire J.-L. Lagrange, Observatoire de la Côte d'Azur (OCA), Université de Nice-Sophia Antipolis (UNS), CNRS, Campus Valrose, 06108, Nice Cedex 2, France
[24]Department of Physics and Astronomy, The University of Oklahoma, 440 W. Brooks St., Norman, OK, 73019, USA

This excesses were subsequently attributed to the presence of cold dust disks. While IR photometry remains the best way to detect new dust disks[11], recent advances enable high-contrast imaging observations at visible and near-IR wavelengths to resolve the spatial architecture of these disks by detecting starlight scattered off dust grains. In addition, high-contrast imaging has discovered a handful of giant planets around stars with debris disks, corroborating the natural link between disks and planets[12–15].

Most debris disks observed by direct imaging feature asymmetries such as rings, warps, clumps, offsets, eccentricities, or brightness asymmetries. These observed structures are often considered to be the result of gravitational perturbations caused by the presence of yet unseen planets, an interpretation which proved to be correct in the case of the β Pic system[2,4,16,17].

The debris disk around AU Mic is peculiar in many respects. The star is a cool, flaring[18] M1Ve type dwarf with a 4.9 day rotation period[19] at a distance of only 9.94 ± 0.13 pc[20]. As a member of the β Pic Moving Group, the adopted age of the star is 23 ± 3 Myr[21]. Its extended ($\sim$200 au) edge-on dust disk was first discovered at visible wavelengths using ground based observatories[22]. The current picture of the system assumes a birth ring of planetesimals located at 35–40 au. Beyond this radius, the disk is populated by small dust particles ($> 0.05\,\mu$m)[8], blown away by the stellar wind as opposed to the radiation pressure involved in disks around earlier-type stars[23,24]. Following the discovery image, the system was intensively observed from the ground and space[5–8]. These observations hinted at brightness asymmetries in the intensity profile of the disk at physical separations of 20–40 au. Most were located in the fainter, southeast side of the disk while the northwest side was more uniform and approximately twice as bright. Observations obtained in August 2010 and July 2011 using HST confirmed these asymmetries[10].

AU Mic was one of the prime test targets during the commissioning of SPHERE, the planet finder instrument installed at the VLT[9]. It was observed on August 10th, 2014, in the J band (1.25μm) with the near IR camera IRDIS. The disk is detected out to $7''$ ($\sim$70 au), as limited by the detector field of view, and as close as $0.17''$ ($\sim$1.7 au), below which the disk is attenuated by the coronagraph (Fig. 1). We measured a position angle (PA) of $129.5^\circ \pm 0.3^\circ$ in the southeast side. The northwest side PA differs by $1.7^\circ \pm 0.4^\circ$ (see Supplementary Information, SI). While the general shape agrees with previous observations, the new SPHERE images show the morphology of the whole disk with unprecedented resolution and detail. In this paper, we focus on the enigmatic patterns in the southeast side. In total, we identified five structures at approximately $1.02''$, $1.70''$, $2.96''$, $4.10''$, $5.52''$ corresponding to physical separations of $\sim$10 to 55 au (see SI). Figure 2 plots the positions of the photometric centroids along the disk (its spine) and identifies the locations of the five structures annotated A to E. The features get fainter, broader, and closer to the mid plane with increasing stellocentric distance. The typical projected sizes of the features range between $\sim$5 to 10 au from inside to outside while they culminate above the disk midplane at $\sim$1.5 to 0.5 au, respectively.

The structures feature arch-like or wave-like morphology unlike anything previously observed in circumstellar disks. Features A and B fall into the field of view of ZIMPOL, the visible light arm of SPHERE, where they are recovered as well (see SI).

In older observations by HST/STIS in 2010/2011 a prominent structure was reported in the southeast side at a projected separation of $\sim$13 au[10]. We re-analyzed these data to yield separate images for the 2010 and 2011 epochs. Both show that this bump is equivalent with feature B seen in the 2014 SPHERE image but situated $\sim$4 au closer to the star (Fig. 1). In fact, the HST re-processed images contain further features at larger separations. A careful analysis reveals that the features in the SPHERE and HST images match with high fidelity across all three epochs (Figure 2). Feature A would be obscured by the coronagraph in 2010. However, all structures identified in 2014 appear to have moved away from the star toward the southeast direction as a coherent train of patterns. From these measurements, we derived the projected speeds of each feature (Figure 3). The motions are faster (>4–11 km/s) than those expected for circular orbits and are found to exceed local escape velocity for at least the three outermost structures, indicating they are unbound and thus are being expelled from the system. The velocities follow a linear trend where the most distance features move faster. However, these distant features are also broader, fainter, and thus more difficult to register with accuracy. The trends are demonstrated in Figure 3 which reinforces the idea of coherence between these structures possibly pointing to a common origin, although we note that features A and B are still compatible with highly eccentric Keplerian orbits.

The fast motion is also illustrated in Fig. 4, which plots the stellocentric distance versus time for each feature. The structures are well aligned over the three epochs, error bars being smaller than the plotted symbols in some cases. Once the data points are fitted with linear trends and extended back in time, three out of five features (A, B, C) lie on nearly parallel tracks, suggestive of a common origin. Interestingly, brightness asymmetries reported in the literature in 2004 coincide with the tracks for features C and D, though it is difficult to determine reliably if they are the same features.

The interpretation of these fast-moving structures in the AU Mic system is rendered difficult by the edge-on view and the short temporal baseline, as well as the lack of observational precedent or theoretical predictions for such phenomena. Most scenarios that we considered are not fully compliant with all the features characteristics. We discuss the various scenarios in the SI. There are mandatory observational facts that a scenario must explain, at least qualitatively, which are: 1) spatial localization, 2) timeframe, 3) increase of projected speeds at larger projected separations, 4) larger projected widths away from the star, 5) increase of intensities at shorter projected separations, 6) decrease of elevations outwards. Having considered several scenarios we speculated that an unseen planet traveling on a fraction of its orbit during the observational timeframe could explain the main characteristics. Potentially triggered by the stellar flares,

episodic outflows pointed away from the star could have been released by this planet, thus leading to the formation of discrete structures in the dust population. The sum of the outflow velocity and the planet velocity vectors changes along the orbit and we observe its projection. In this picture, feature E is the oldest and the most distant from the star while feature A is directed towards the observer. Given that features A and E could have been released ∼15 years apart (Fig. 4) and that projected speeds vary from ∼4 to 10 km/s (Fig. 3), this simple model allows us to constrain the minimal separation of a planet to ∼10–15 au. On the other side, dust clearing observed at distances closer than ∼35–40 au could be the result of a planet orbiting inside the planetesimals belt[23]. In the range 10–40 au the SPHERE data reach a contrast of 1.10^{-6} to 8.10^{-8}, which, depending on evolutionary models[25,26], places an upper limit at 6–3.5 Jupiter masses, respectively. An inclined orbit could help to account for the decreasing elevations of the features.

Several mechanisms could be responsible for a planetary outflow. In that respect, stellar winds or flares, of which the effect is attested for AU Mic, should play an important role. For instance, atmospheric escape is common for Hot Jupiter planets and produces cometary tail-like structures[27]. Another case of interest may involve the presence of a planetary magnetosphere. Planetary magnetic field lines reconnect with the magnetized stellar wind creating a magnetotail which can lead to cyclical ejections of plasma out of the tail[28]. Dust particles interacting with the ejected plasma are accelerated by the Lorentz force which is dominant over gravity. This would yield an outflow pointed away from the star, and may explain the super-Keplerian velocities of a few tens of km/s[29,30] and possibly vertical transport with respect to the disk midplane. Such magnetotail ejections are observed in the solar system from Jupiter and Saturn 1–2 au away from the planet. For the time being, our observations cannot discriminate between these different physical scenarios, though as we discuss in the SI, imaging polarimetry and monitoring observations have the potential to break some of these degeneracies in the coming years.

References

[1] Backman, D. E. & Paresce, F. Main-sequence stars with circumstellar solid material - The VEGA

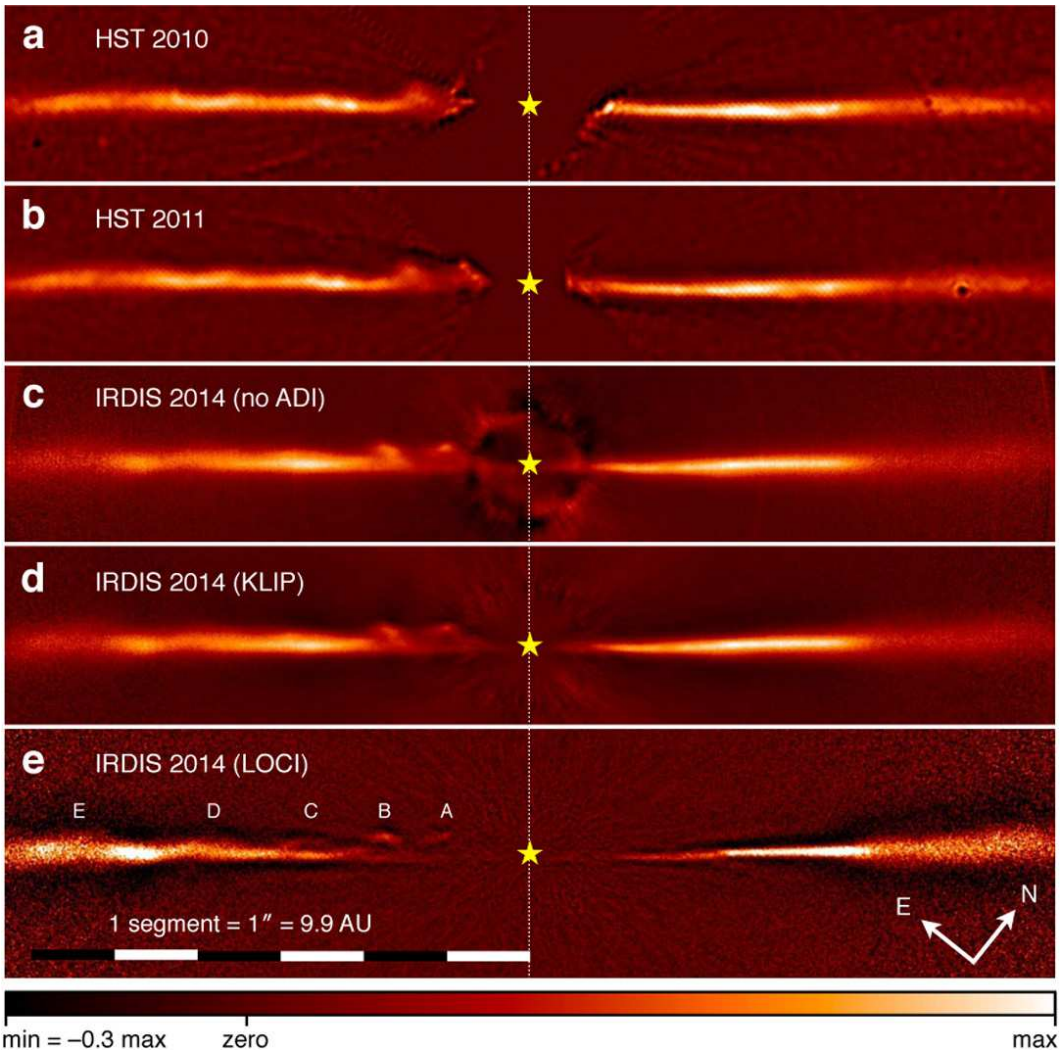

Figure 1: **High-contrast images of the AU Mic debris disk**. Images are shown for the 3 epochs (2010.69, 2011.63, 2014.69) at the same spatial scale the location of AU Mic marked with a yellow star symbol. In the two upper panels (a, b) the HST/STIS data were processed with roll subtraction and high-pass filtered to reveal the various features. SPHERE/IRDIS images are displayed in panels c, d, and e, for three differential imaging techniques (see SI for details). The intensity maps are multiplied by the square of the stellocentric distance to counteract the high dynamic range of the data and make the disk structures visible at all separations. Therefore, the disk in the central area is in fact brighter than it appears (see SI for a linear intensity stretch). The color scale represents different absolute intensity ranges in the images to account for the varying degree of flux loss in the different processing techniques, but the ratio of minimum to maximum value is kept constant.

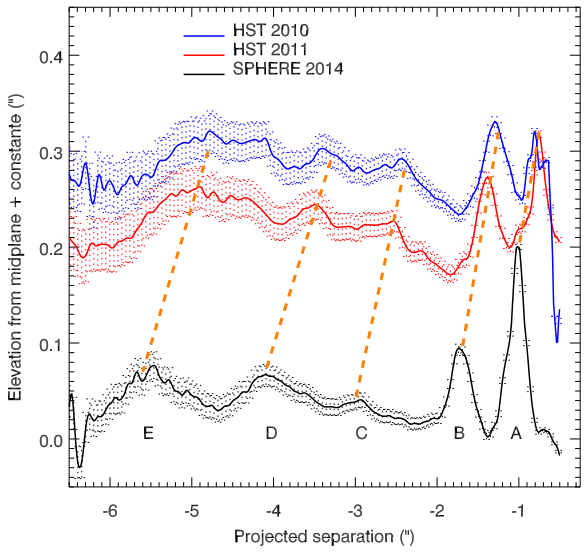

Figure 2: **Matching disk features across three epochs of observation.** For each of the three disk images, we plot the vertical position of the disk's spine (photometric centroid) as a function of radial distance to the star. For the sake of clarity, the profiles are shifted vertically in proportion to the time intervals between epochs. We identify a recurring pattern of five local maxima (marked A–E) corresponding to the visually identified wave-like features. Dashed orange lines roughly illustrate the possible trajectory of each feature. Note that feature A is fully obscured by the coronagraph in 2010, and at least partly so in 2011. Errors in the profiles are dominated by the uncertainty on the disk position angle (0.3°–0.5°).

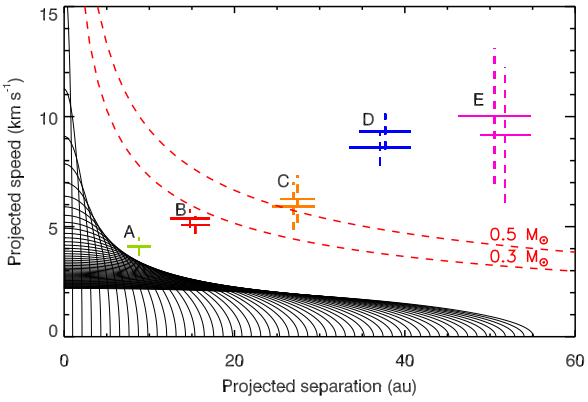

Figure 3: **Projected speeds of the disk features.** The projected speeds of the five features A–E (green, red, orange, blue, magenta) are plotted against the projected distance from the star, revealing a trend of increasing speed with increasing distance. The three epochs yield three projected separations and two projected speeds (we did not consider the speed between the two HST image as the time baseline is too short), except for feature A, undetected in 2010. The family of solid black curves shows circular Keplerian orbits viewed edge-on for comparison (calculated for 0.3 solar mass) . The dotted red curves show the maximum local system escape speed as a function of projected distance from the star for two different assumptions on the mass of AU Mic (0.3 and 0.5 solar mass); thus, any object above this curve cannot be gravitationally bound to AU Mic. All observed features exhibit projected speeds in excess of expectations from circular orbits, and at least three (C–E) are on unbound trajectories.

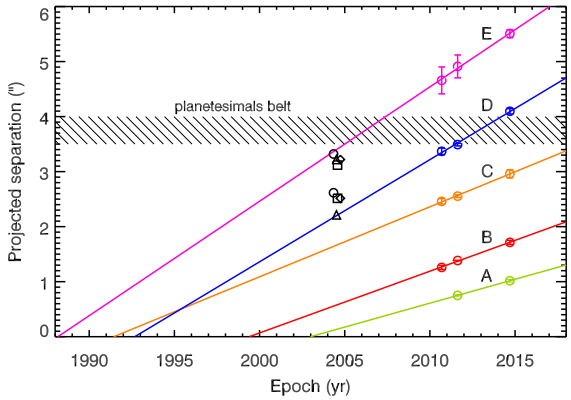

Figure 4: **Positions of the disk features over time.** Positions of features measured in SPHERE and HST images are plotted as diamonds together with error bars (in some cases, the errors are smaller than the symbol size). Linear fits on these three epochs illustrate the possible track of each feature. The black symbols show the location at which inhomogeneities were reported in literature based on older data[5–8]. The color coding is the same as in Figure 3.

phenomenon. In Levy, E. H. & Lunine, J. I. (eds.) *Protostars and Planets III*, 1253–1304 (1993).

[2] Mouillet, D., Larwood, J. D., Papaloizou, J. C. B. & Lagrange, A. M. A planet on an inclined orbit as an explanation of the warp in the Beta Pictoris disc. *Mon. Not. R. Astron. Soc.* **292**, 896 (1997).

[3] Ozernoy, L. M., Gorkavyi, N. N., Mather, J. C. & Taidakova, T. A. Signatures of Exosolar Planets in Dust Debris Disks. *Astrophys. J.* **537**, L147–L151 (2000).

[4] Lagrange, A.-M. *et al.* The position of β Pictoris b position relative to the debris disk. *Astron. Astrophys.* **542**, A40 (2012).

[5] Liu, M. C. Substructure in the Circumstellar Disk Around the Young Star AU Microscopii. *Science* **305**, 1442–1444 (2004).

[6] Metchev, S. A., Eisner, J. A., Hillenbrand, L. A. & Wolf, S. Adaptive Optics Imaging of the AU Microscopii Circumstellar Disk: Evidence for Dynamical Evolution. *Astrophys. J.* **622**, 451–462 (2005).

[7] Krist, J. E. *et al.* Hubble Space Telescope Advanced Camera for Surveys Coronagraphic Imaging of the AU Microscopii Debris Disk. *Astron. J.* **129**, 1008–1017 (2005).

[8] Fitzgerald, M. P., Kalas, P. G., Duchêne, G., Pinte, C. & Graham, J. R. The AU Microscopii Debris Disk: Multiwavelength Imaging and Modeling. *Astrophys. J.* **670**, 536–556 (2007).

[9] Beuzit, J.-L. *et al.* SPHERE: a 'Planet Finder' instrument for the VLT. In *Society of Photo-Optical Instrumentation Engineers (SPIE) Conference Series*, vol. 7014, 18 (2008).

[10] Schneider, G. *et al.* Probing for Exoplanets Hiding in Dusty Debris Disks: Disk Imaging, Characterization, and Exploration with HST/STIS Multi-roll Coronagraphy. *Astron. J.* **148**, 59 (2014).

[11] Eiroa, C. *et al.* DUst around NEarby Stars. The survey observational results. *Astron. Astrophys.* **555**, A11 (2013).

[12] Marois, C. *et al.* Direct Imaging of Multiple Planets Orbiting the Star HR 8799. *Science* **322**, 1348–1352 (2008).

[13] Kalas, P. *et al.* Optical Images of an Exosolar Planet 25 Light-Years from Earth. *Science* **322**, 1345– (2008).

[14] Lagrange, A. M. *et al.* A Giant Planet Imaged in the Disk of the Young Star Pictoris. *Science* **329**, 57–59 (2010).

[15] Rameau, J. *et al.* Confirmation of the Planet around HD 95086 by Direct Imaging. *Astrophys. J. Letters* **779**, L26 (2013).

[16] Augereau, J. C., Nelson, R. P., Lagrange, A. M., Papaloizou, J. C. B. & Mouillet, D. Dynamical modeling of large scale asymmetries in the beta Pictoris dust disk. *Astron. Astrophys.* **370**, 447–455 (2001).

[17] Lagrange, A. M. *et al.* An insight in the surroundings of HR 4796. *Astron. Astrophys.* **546**, 38 (2012).

[18] Robinson, R. D., Linsky, J. L., Woodgate, B. E. & Timothy, J. G. Far-Ultraviolet Observations of Flares on the dM0e Star AU Microscopii. *Astrophys. J.* **554**, 368–382 (2001).

[19] Plavchan, P. *et al.* New Debris Disks Around Young, Low-Mass Stars Discovered with the Spitzer Space Telescope. *Astrophys. J.* **698**, 1068–1094 (2009).

[20] Perryman, M. A. C. *et al.* The HIPPARCOS Catalogue. *Astron. Astrophys.* **323**, L49–L52 (1997).

[21] Mamajek, E. E. & Bell, C. P. M. On the age of the β Pictoris moving group. *Mon. Not. R. Astron. Soc.* **445**, 2169–2180 (2014).

[22] Kalas, P., Liu, M. C. & Matthews, B. C. Discovery of a Large Dust Disk Around the Nearby Star AU Microscopii. *Science* **303**, 1990–1992 (2004).

[23] Augereau, J. C. & Beust, H. On the AU Microscopii debris disk. *Astron. Astrophys.* **455**, 987–999 (2006).

[24] Strubbe, L. E. & Chiang, E. I. Dust Dynamics, Surface Brightness Profiles, and Thermal Spectra of Debris Disks: The Case of AU Microscopii. *Astrophys. J.* **648**, 652–665 (2006).

[25] Chabrier, G. & Baraffe, I. Theory of Low-Mass Stars and Substellar Objects. *Ann. Rev. Astron. Astrophys.* **38**, 337–377 (2000).

[26] Baraffe, I., Chabrier, G., Barman, T. S., Allard, F. & Hauschildt, P. H. Evolutionary models for cool brown dwarfs and extrasolar giant planets. The case of HD 209458. *Astron. Astrophys.* **402**, 701–712 (2003).

[27] Matsakos, T., Uribe, A. & Königl, A. Classification of magnetized star–planet interactions: bow shocks, tails, and inspiraling flows. *arXiv.org* (2015). `1503.03551v1`.

[28] Vogt, M. F., Kivelson, M. G., Khurana, K. K., Joy, S. P. & Walker, R. J. Reconnection and flows in the Jovian magnetotail as inferred from magnetometer observations. *J. Geophys. Res.* **115**, 6219 (2010).

[29] Kivelson, M. G. & Southwood, D. J. Dynamical consequences of two modes of centrifugal instability in Jupiter's outer magnetosphere. *J. Geophys. Res.* **110**, A12209 (2005).

[30] Hsu, H.-W. *et al.* Stream particles as the probe of the dust-plasma-magnetosphere interaction at Saturn. *J. Geophys. Res.* **116**, 9215 (2011).

Supplementary Information is linked to the online version of the paper available at www.nature.com/nature.

Acknowledgements SPHERE is an instrument designed and built by a consortium consisting of IPAG (Grenoble, France), MPIA (Heidelberg, Germany), LAM (Marseille, France), LESIA (Paris, France), Laboratoire Lagrange (Nice, France), INAF - Osservatorio di Padova (Italy), Observatoire de Geneve (Switzerland), ETH Zurich (Switzerland), NOVA (Netherlands), ONERA (France) and ASTRON (Netherlands), in collaboration with ESO. SPHERE was funded by ESO, with additional contributions from CNRS (France), MPIA (Germany), INAF (Italy), FINES (Switzerland) and NOVA (Netherlands). SPHERE also received funding from the European Commission Sixth and Seventh Framework Programmes as part of the Optical Infrared Coordination Network for Astronomy (OPTICON) under grant number RII3-Ct-2004-001566 for FP6 (2004-2008), grant number 226604 for FP7 (2009-2012) and grant number 312430 for FP7 (2013-2016). This study is based on observations made with the NASA/ESA Hubble Space Telescope, obtained at the Space Telescope Science Institute, which is operated by the Association of Universities for Research in Astronomy, Inc., under NASA contract NAS 5-26555. These observations are associated with program # 12228.

Support for program # 12228 was provided by NASA through a grant from the Space Telescope Science Institute, which is operated by the Association of Universities for Research in Astronomy, Inc., under NASA contract NAS 5- 26555. CG was partially supported through the NASA Origins of Solar Systems Program on NNG13PB64P, while JP was supported under NNX13AK17G. We are also grateful to ESO for releasing the commissioning data for publication. Finally, we thank P. Zarka., N. Meyer-Vernet, B. Stelzer and Q. Kral for helpful discussions.